JOURNAL OF AGRICULTURAL AND FOOD CHEMISTRY

Synthesis, Rheological Characterization, and Constitutive Modeling of Polyhydroxy Triglycerides Derived from Milkweed Oil

R. E. HARRY-O'KURU*,† AND C. J. CARRIERE‡

New Crops and Processing Technology Research and Cereal Products & Food Science Research Unit, National Center for Agricultural Utilization Research, Agricultural Research Service, USDA, 1815 North University Street, Peoria, Illinois 61604

Asclepias syriaca L., the common milkweed, is a new industrial crop. The seed contains about 20−30 wt % of a highly unsaturated oil having unusual fatty acids. Exploring value-added products from the oil, milkweed trglycerides have been oxidized by in situ performic acid to the polyoxirane and polyhydroxy triglycerides (PHTG). The rheological properties of milkweed PHTG were characterized in various shear flows. Milkweed PHTG displayed nonlinear viscoelastic behavior at applied strains greater than 1%. Milkweed PHTG was found to obey time−strain separability. A nonlinear Wagner constitutive model was used successfully to qualitatively predict the behavior of milkweed PHTG in both start-up and cessation of steady-state shear flow.

KEYWORDS: Milkweed oil; epoxidation; polyhydroxyl triglyceride; rheology

INTRODUCTION

Asclepias syriaca L. species of the family Asclepiadaceae, otherwise known as the common milkweed, is found mainly between the Rocky and Appalachian Mountain ranges of the United States and from southern Canada to northern Mexico. It tends to thrive copiously in crop fields and so is considered a pest by most farmers. However, milkweed is now an industrial crop. Its inflorescence produces clusters of pods which, when mature, generate three product types: a fine silky fiber, seed, and pod hulls. The hypoallergenic fiber is currently being used in pillows and comforters.

The seed has about 25% oil content. The oil-free seed meal is a potent nematicide and pesticide against army worms (*1*). Even the pod hulls have nematicidal activity. Milkweed oil has been shown to be highly unsaturated (*2*), and cardenolide-free (*3*). At present, this vegetable oil cannot successfully compete as an edible oil because of the small acreage of the cultivated crop. It could, however, fare very well in a low-volume, value-added, niche market when the oil is appropriately functionalized beyond the olefinic moieties. In recent years increased new industrial uses of vegetable oils as renewable feedstock with biodegradable characteristics have evolved following chemical and or enzymic modification of the methyl esters or carboxylic acids of traditional commodity crop seed oils (*4*−*9*).

The advent of unique new crop oils bearing epoxy groups, e.g., *Vernonia galamensis* seed, (*10*) or hydroxyl triglycerides (*11*) will be changing the traditional uses of vegetable oils. Like castor oil, these new crop oils will lend themselves to a variety of new industrial applications. We now report a study of the rheological properties of milkweed polyhydroxy triglyceride (PHTG) generated in an in situ performic acid oxidation of milkweed oil (*12*). The flow behavior of this material has been compared to those of castor oil, "the industrial gold standard" of hydroxy vegetable oils, and the starting milkweed triglyceride.

MATERIALS AND METHODS

Materials and Reagents. Crude, cold-pressed milkweed oil was obtained from Natural Fibers Corporation (Ogallala, NE). Activated acid clay (bentonite) was obtained from Harshaw/Filtrol Clay Products Division (Jackson, MS). Sample centrifugation was performed using a Beckman Coulter centrifuge, model J2-HS (Beckman Coulter, Inc., Fullerton, CA). Formic acid (90.4% and 99.0%) was obtained from Fisher Scientific (Chicago, IL) and hydrogen peroxide 50% in water was from Aldrich Chemical Co. (St. Louis, MO). Castor oil was purchased from a local pharmacy. FTIR spectra were recorded on a Bomem MB-Series FTIR, (Bomem, Quebec, PQ) and ^{1}H and ^{13}C NMR spectra were obtained on a Bruker ARX-400 with a 5-mm dual proton/carbon probe (Bruker Spectrospin, Ballerica, MA), using tetramethylsilane as internal standard. Specific rotation $[\alpha]_D^{20}$ values were measured on a Perkin-Elmer Polarimeter model 341 (Perkin-Elmer, Norwalk, CT). Kinematic viscosities were measured on a Cannon viscometer with the 400 (378E) or 300 tubes in a Temp-Trol Viscosity Bath, (Precision Scientific, Chicago, IL).

Synthesis of Epoxy Triglyceride. In a typical process, reprocessed milkweed oil (582.0 g, 673.76 mmol), iodine value = 111.4, $[\alpha]_D^{20} = +0.11°$, was placed in a 1-L, three-necked jacketed flask equipped with a mechanical stirrer and was heated to 45.5 °C. Formic acid (99%, 39.7 g, 0.3 equiv/mol of C═C) was added, and the mixture was stirred to homogeneity. Hydrogen peroxide (50%, 320 mL, 6.74 mol) was then added slowly (i.e., dropwise). At the end of hydrogen peroxide

* To whom correspondence should be addressed (telephone +309 681 6341; fax +309 681 6524; e-mail harryore@ncaur.usda.gov.
† New Crops and Processing Technology Research.
‡ Cereal Products & Food Science Research Unit.

10.1021/jf011464z
Published on Web 04/30/2002

addition, the temperature was raised to 70 °C and vigorous stirring was continued for 7 h. The heat source was then removed, the reaction mixture was allowed to cool, and the mixture was transferred to a separatory funnel with ethyl acetate as diluent. The material was washed with saturated NaCl (300 mL × 4) followed by saturated Na_2CO_3 (40 mL) in additional NaCl solution. When a pH of 7.5 was reached, the organic phase was then washed with deionized water. The wet organic layer was separated from a turbid aqueous phase and was concentrated at 60 °C in vacuo to remove the solvent and water. The yield of epoxy triglyceride was 558.4 g; the measured kinematic viscosities were 1209 centistokes (cSt) at 40 °C and 81.3 cs at 100 °C; PV = 9.4, IV = 1.79. The specific rotation was $[\alpha]_D^{20} = +0.17°$ An aqueous fraction (42.0 g) was reclaimed from the final water-wash following concentration at 70 °C, to give a total yield of 600.6 g (97%). IR values were (film on KBr, main fraction) cm^{-1}: 3471 w, 2927 vs, 2856 vs, 1743 vs, 1560 w, 1463 s, 1375 s, 1242 s, 1162 s, 1105 s, 1048 s, 824−842 d(m), 726 w-m. IR (minor fraction) cm^{-1}: 3455 s, 2926 vs, 2855 s, 1743 vs, 1560 w, 1463 m, 1380 m, 1255 m, 1162 m-s, 1106 m, 824−842 d (w), 725 d (w-m). ^1H NMR (main fraction in $CDCl_3$) δ: 5.25 m (residual vinylic), 4.29 dd (J = 4.3, 11.9 Hz, 2H), 4.14 dd (J = 5.9, 11.9 Hz, 2H), 3.1 m (2H), 2.96 m (2H), 2.89 m (2H), 2.3 m (6H), 1.75−1.25 m (72H), 0.87 m (9H). ^{13}C ($CDCl_3$) δ: 173.1, 172.7, 68.87, 62.02, 57.10, 57.05, 56.91, 56.85, 56.63, 56.55, 54.25, 54.09, 34.06, 33.90, 31.79, 31.61, 29.63, 29.47, 29.28, 29.23, 29.15, 29.12, 28.92, 28.88, 27.83, 27.77, 27.75, 27.16, 26.88, 26.55, 26.52, 26.08, 24.73, 22.51, 13.93.

Synthesis of Polyhydroxy Triglycerides. Reprocessed milkweed oil (3430.0 g, 3.971 mol, IV = 128.5) in a 12-L three-necked jacketed flask was stirred vigorously at 40 °C and formic acid (99.0%, 511.77 g, 11.12 mol) was added in one portion followed with a slow addition of H_2O_2 (50%, 2837.0 g, 61.64 mol). At the end of peroxide addition, the temperature was increased to 70 °C. After 15 h, the heat source was removed, and stirring was continued to allow the reaction mixture to cool to room temperature, after which the aqueous phase was removed. Deionized water (2000 mL) was added and followed with 12.1 M HCl (300 mL). The nearly colorless sludge was stirred at 70 °C overnight. The cream-colored product was transferred into a separatory funnel using ethyl acetate as diluent. The aqueous layer was discarded, and the organic phase was washed sequentially with saturated NaCl solution, saturated $NaHCO_3$ to a pH of 7.5, and deionized water. Ethanol was added to facilitate separation of the phases. After removal of the aqueous layer, the product was vacuum concentrated at 50 °C. The yield was 3924.0 g (96.6%) of the polyhydroxyl triglyceride with an iodine value of 14 compared to an iodine value of 128.5 in the starting milkweed oil. The measured kinematic viscosities were 3710 cSt at 40 °C and 101.7 cSt at 100 °C, i.e., a viscosity index VI = 88. Specific rotation $[\alpha]_D^{20} = +0.37°$. IR (film on KBr) cm^{-1}: 3636−3168 b, 2927 vs, 2856 vs, 1743 vs, 1463 s, 1378 m-s, 1240 m-s, 1173 vs, 1097 s, 881 w, 725 w-m. ^{13}C NMR ($CDCl_3$) δ: 173.2, 172.8, 84.60, 83.00, 82.50, 82.00, 80.50, 74.40, 73.82, 73.20, 68.82, 62.04, 34.75, 34.48, 34.10, 33.94, 33.54, 31.79, 31.61, 30.47, 29.64, 29.56, 29.47, 29.42, 29.31, 29.26, 29.21, 29.17, 29.05, 28.91, 25.58, 25.26, 24.76, 22.61, 22.56, 22.45, 14.08.

Acetylation of Polyhydroxy Triglyceride. Polyhydroxy triglyceride (8.90 g, 9.95 mmol) was placed in a dry 100-mL round-bottomed flask containing a magnetic stir bar and fitted with a rubber septum. Reagent-grade acetic anhydride (40.0 mL) and dry Et_3N (5.0 mL) were added via a syringe. The mixture was stirred at room temperature (36 h) and then poured into a 500-mL beaker containing 150 mL of ethyl acetate. The reaction flask was rinsed twice with 40 mL of additional ethyl acetate, and the combined solution was stirred with satd $NaHCO_3$ (250 mL) until effervescence ceased. The mixture was then transferred into a separatory funnel, and the aqueous layer was removed and discarded. The organic phase was washed with deionized water, dried ($NaSO_4$), and concentrated in vacuo to give 9.5 g (77.6%) of the acetate ester of the triglyceride. IR (smear on KBr) cm^{-1}: 2928 s, 2857 m-s, 1742 vs, 1462 m, 1372 m, 1235 s, 1171 m-s, 1100 m, 1026 m, 952 w, 725 w. ^{13}C NMR ($CDCl_3$) δ: 173.1, 172.7, 170.1, 160.4, 77.25, 75.05, 73.77, 73.50, 68.83, 65.74, 63.25, 62.00, 35.06, 34.03, 33.87, 31.74, 30.66, 30.59, 29.61, 29.57, 29.53, 29.38, 29.28, 29.23, 29.18, 29.09, 29.02, 28.98, 28.87, 24.98, 24.77, 24.68, 22.56, 22.40, 20.84, 15.19, 14.01, 13.90.

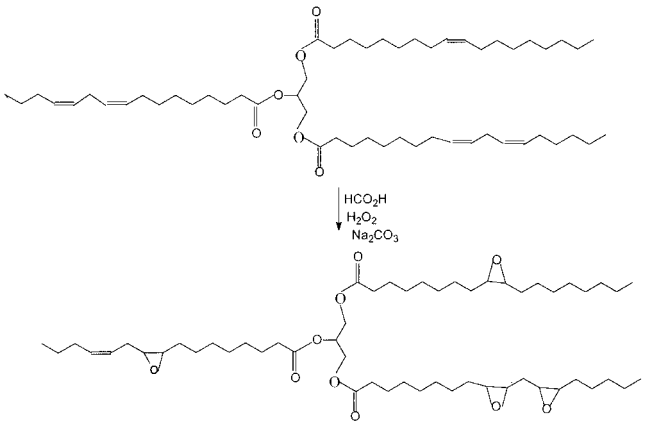

Figure 1. Formation of tetra epoxy triglyceride of refined *A. syriaca* oil.

Rheological Methods. Rheological properties were measured using a Rheometrics ARES Series V controlled-strain rheometer with a cone-and-plate fixture operating under Rheometrics Orchestrator version 6.4.3 software. All the rheological studies were conducted using a 50-mm diameter, 0.0401-radian cone with a 0.046-mm gap. The temperature of the sample was controlled using a jacketed circulating water bath which enabled the chamber of the viscometer to be controlled to better than ± 0.1 °C. All the experiments reported herein were conducted at 25 °C. Several different rheological experiments were carried out on the various materials. Rate sweep experiments were conducted with shear rates ranging from 10^{-4} to 100 s^{-1}. Oscillatory shear experiments were performed with applied strains of 0.2, 1, 2, 5, 20, and 50% and a frequency range of 0.01 to 100 rad/s. Stress relaxation experiments were executed with applied strains of 0.2, 1, 2, 5, 20, and 50% and an experiment time of 10^3 s. Start-up of steady-state shear experiments were performed with applied shear rates of 0.001, 0.01, 0.1, and 1 s^{-1} using a hold time between changes in the applied shear rate of 600 s. Cessation of steady-state shear experiments were carried out at applied shear rates of 0.001 and 0.01 s^{-1} with hold times of 600 s between the changes in the applied shear rate and after the cessation of the applied shear.

The fits to the experimental data and calculations for the constitutive model predictions were performed using Mathsoft MathCad 6.0 and Waterloo Maple V software running on a 466-MHz Apple Macintosh G3 computer. Graphical presentations of the data and model predictions were generated using Wavemetrics Igor Pro 3.15 software.

RESULTS AND DISCUSSION

Epoxy Triglyceride. The oxidation of olefinic bonds of unsaturated fatty acids and their methyl esters using organic peracids, namely, the Prileschajew reaction, has been intensely studied and reviewed (*8*, *13*) because of the latent potential of triglycerides as renewable industrial feedstock from vegetable oils. During the exploratory stage of this study to determine methods suitable to milkweed oil oxidation we investigated several methods including the chemoenzymic approach (*14*, *15*). Although these processes were moderately successful without optimization, an alternative and cost-effective oxidation system was sought that would more satisfactorily address the special needs of milkweed oil. Thus, in a modification of the in situ performic acid oxidation method reported (*5*, *16*), the oxidation of refined milkweed triglycerides resulted in almost quantitative yields of the oxirane triglycerides when 0.4 equiv formic acid and 3.0 mol of H_2O_2 per mol of carbon−carbon double bond were employed under neat reaction conditions, as shown in **Figure 1**. Its ^{13}C NMR chemical shifts data show eight carbon resonances at δ 57.01, 57.05, 56.91, 56.85, 56.63, 56.55, 54.25,

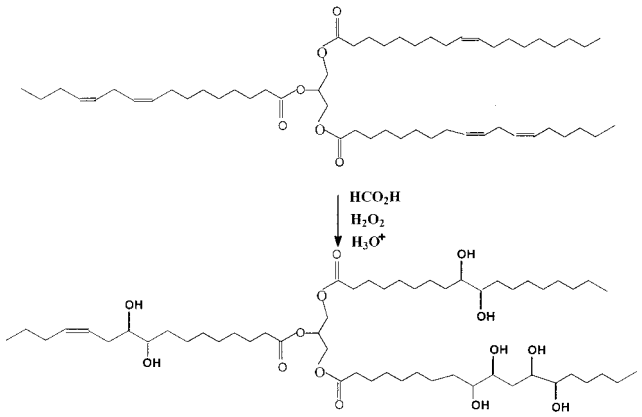

Figure 2. One-pot conversion of refined *A. syriaca* oil to the polyhydroxy triglyceride.

and 54.09 ppm, ascribable to the epoxy ring carbons. Because epoxidation is a stereospecific addition reaction to the C−C double bonds which have cis configuration in the natural triglyceride, the reaction product is the cis tetra-oxirane compound based on the data. This is consistent with published literature (*17*). Two other ^{13}C resonances are the primary C1, C3 of the esterified glycerol moiety that are chemically and magnetically equivalent and therefore overlap at δ 62.02 ppm while its C2 is observed at δ 68.87 ppm. Although the ^{13}C NMR of this product gave no resonances corresponding to olefinic carbons, the ^{1}H spectrum of the same sample does indicate some residual vinylic proton(s) suggesting that the product was not completely epoxidized. This is not surprising considering the level of unsaturation in the starting triglyceride.

The Fourier transform−IR (FTIR) spectrum of this product shows the characteristic doublet at 824−842 cm^{-1} of the C−O−C oxirane stretch usually observed in the naturally epoxidized vegetable oils (*10*). An inherent feature of peracid epoxidation, however, is the intrinsic acid strength of the acid, which tends to cause some oxirane ring-opening to the diols as previously noted (*13*) in acetic acid solvents and in performic acid (*16*). The epoxy ring-opening was not a serious drawback, as our target product was the polyhydroxy triglycerides. When the epoxide is the sole product desired, the reaction conditions and progress could be strictly timed and monitored so as to be quenched at the optimum moment with the least amount of diol formation. The physical properties of the tetra-oxirane triglycerides include a high kinematic viscosity of 1209 cSt, an epoxide value of 9.4, and an iodine value of 1.79 compared to 111.4 for the parent oil.

Polyhydroxy Triglyceride. The polyhydroxy triglyceride was synthesized in a single step, without preseparation of the intermediate epoxide, **Figure 2**. The process was high-yielding, giving a material of unique properties. The presence of several pendant hydroxyl groups gives this compound the ability to form inter- and intramolecular hydrogen bonds. Besides hydrogen bonding, the pendant substituents on the main chains impart tacky behavior to the bulk material as they entangle with each other (*18*). These characteristics manifest a very high kinematic viscosity (3710 cSt at 40 °C and 101.7 cSt at 100 °C). The much lower viscosity observed at 100 °C confirms the role played by hydrogen-bonding in the behavior of this compound.

The IR spectral features of this compound are the broad O−H stretching mode at 3168−3636 cm^{-1}, a strong ester carbonyl band at 1743 cm^{-1}, and the disappearance of the H−C═ stretch and C═C breathing modes of the olefinic starting material. Acetylation of the hydroxyl functions gave much cleaner proton and carbon spectra showing better line resolution. Use of the distortionless enhancement polarization transfer (DEPT) experiment in the spectrum of the acetylated compound enabled resolution of the two primary glycerols C1 and C3 at 62.02 and 65.78 ppm, respectively. The tertiary carbons bearing the acetylated hydroxyls are thus lower field at δ 68.84, 70.05, 73.42, 73.79, 75.03, 77.50, 81.02. An interesting characteristic of the polyhydroxy triglyceride is its moisture holding capacity. When the final workup does not include use of an organic solvent, the isolated PHTG product is usually turbid even after heating overnight at 70 °C under vacuum in a desiccating process. The compound under this condition is referred to as hydrated PHTG and forms very stable emulsions when a 50/50 wt % mixture of it in water is agitated (*12*).

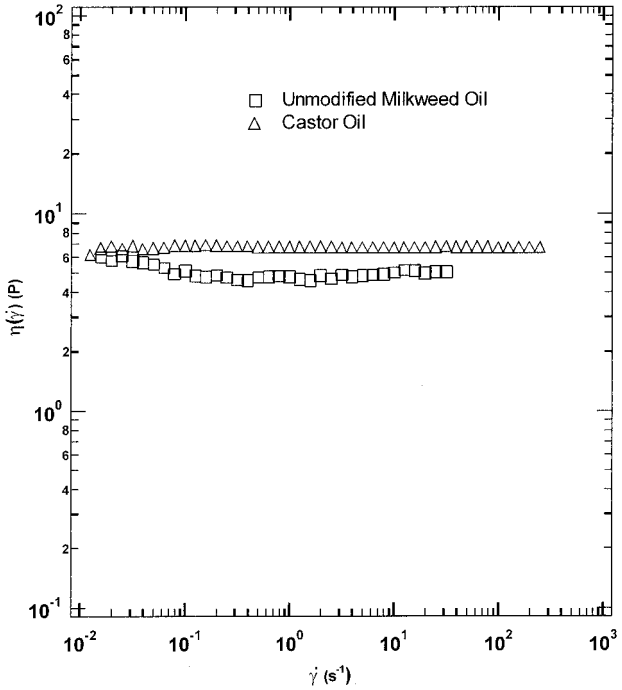

Figure 3. Effect of shear rate on the viscosity of castor oil and unmodified milkweed oil at 25 °C. Newtonian behavior is exhibited by both of the materials across the shear rate range.

Rheological Behavior of Castor Oil and Unmodified Milkweed Oil. The responses of castor oil and unmodified milkweed oil to an applied shear rate sweep are illustrated in **Figure 3**. Both of the materials displayed Newtonian behavior, i.e., no dependence of the viscosity, $\eta(\dot{\gamma})$, on the applied shear rate, $\dot{\gamma}$, across the shear rate range studied. Considering both of these materials are low-molecular-weight oils without major hydrogen bonding this result is expected. The castor oil sample has a viscosity of 6.67 ± 0.06 P, whereas the unmodified milkweed oil has a viscosity of 4.97 ± 0.4 P.

Nonlinear Rheological Behavior of Hydrated Milkweed PHTG. In contrast to the observed rheological behavior of castor oil and unmodified milkweed oil, hydrated milkweed PHTG displays non-Newtonian, shear-thinning behavior during a shear rate sweep experiment as illustrated in **Figure 4**. The viscosity of hydrated milkweed PHTG is observed to drop from approximately 10^5 P at a shear rate of 10^{-4} s^{-1} down to approximately 20 P at a shear rate of 100 s^{-1}. At a shear rate of 3 s^{-1}, the shear-thinning behavior of the sample is observed to change with a less pronounced dependence of the viscosity on the applied shear rate. This may be the onset of a shear-thickening region; however, due to experimental difficulties, it was not possible to conduct reliable measurements on the system at

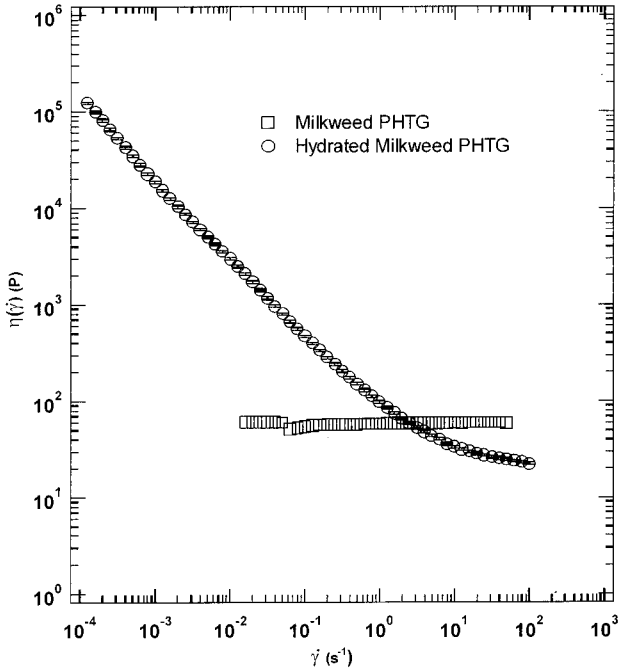

Figure 4. Effect of shear rate on hydrated milkweed PHTG and PHTG at 25 °C. Newtonian behavior is exhibited by the milkweed PHTG sample, whereas hydrated milkweed PHTG exhibits non-Newtonian flow behavior.

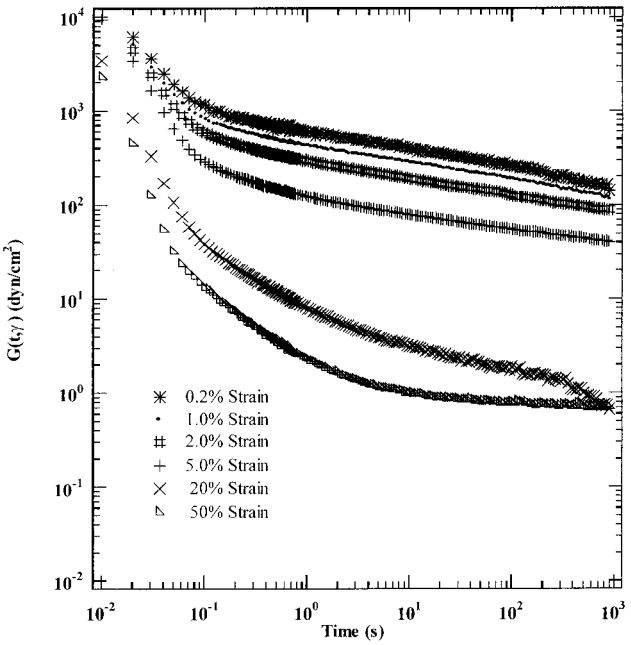

Figure 5. Effect of applied strain on the stress relaxation behavior of hydrated milkweed PHTG at 25 °C.

higher shear rates. Milkweed PHTG displayed Newtonian flow behavior similar to that of castor oil and unmodified milkweed oil (**Figure 4**). The viscosity of the milkweed PHTG sample was 60 ± 3 P.

The hydrated milkweed PHTG material displayed nonlinear rheological behavior at applied strains greater than approximately 1%. This behavior is illustrated in **Figure 5** where the stress relaxation behavior of the fluid is displayed at strains of 0.2, 1, 2, 5, 20, 50%. At strains greater than 1% the stress relaxation modulus, $G(t,\gamma)$, is observed to drop in magnitude with increasing applied strain, γ, indicative of nonlinear viscoelastic (VE) behavior. The stress relaxation modulus drops quickly after the onset of the applied strain. At high applied

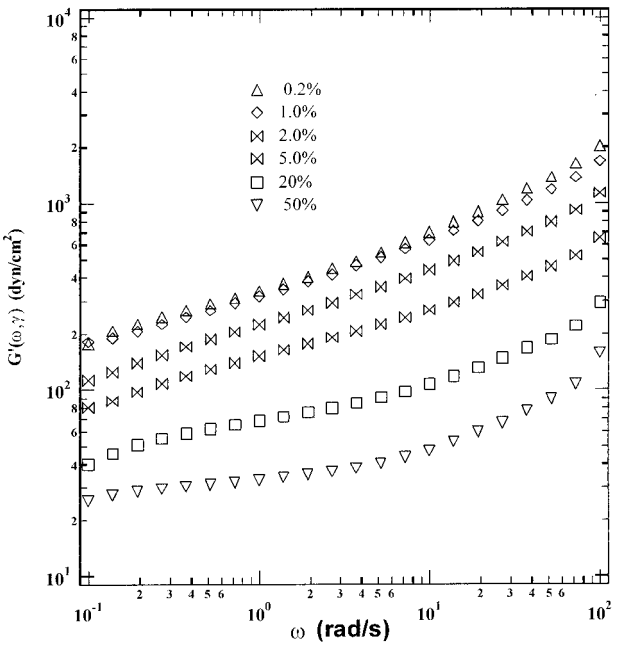

Figure 6. Effect of applied strain on the oscillatory shear modulus of hydrated milkweed PHTG at 25 °C.

strains $G(t,\gamma)$ appears to decay to a plateau; however, this is an artifact of the experiment as the measured torque at 10^3 s is essentially zero (data not displayed).

Similar behavior is observed for the hydrated milkweed PHTG sample in oscillatory shear flow. The effect of shear on the oscillatory shear modulus, $G(\omega,\gamma)$ is illustrated in **Figure 6**. At applied strain amplitudes greater than 1%, $G(\omega,\gamma)$ is observed to decrease as the strain amplitude is increased. Again this is indicative of the nonlinear VE behavior exhibited by hydrated milkweed PHTG. At low shear rates in both the linear and nonlinear VE regimes, the material is observed to approach an apparent plateau region. This may be indicative of a transient network formed in the sample, possibly through entanglements of the chains. Unfortunately, lower frequency measurements were complicated by excessive drying of the sample over the time required to acquire the next decade in frequency response.

A comparison of the data obtained during oscillatory shear flow data and during a rate sweep experiment is illustrated in **Figure 7**. The data follow the Cox−Merz rule (*19*) which states that viscosity of a material obtained during a constant shear experiment should superimpose on the measured complex viscosity, $/\eta^*/$, obtained during an oscillatory shear experiment when $\dot{\gamma} = \omega$ whereω is the oscillatory frequency expressed in s^{-1}. The Cox-Merz rule is an empirical expression. Many systems are known to follow this relationship; however, many biological material and most food systems appear to violate the relationship. Although a direct interpretation of the significance of agreement with, or deviation from, the Cox-Merz rule is not clear, there is some indication that systems that do not follow the rule may possess heterogeneous structure.

Prediction of the Nonlinear Transient Shear Rheology of Hydrated Milkweed PHTG. *Constitutive Model.* The constitutive model used in this work is a modification of the K-BKZ model (*20*) and generally referred to as the Wagner model. The Wagner model may be expressed as follows (*20*−*22*):

$$\tau = -\int_{-\infty}^{t} m(t-t')h(I_B,II_B)B(t')dt' \qquad (1)$$

where τ is the stress dyadic, $B(t')$ is the Finger strain dyadic

Table 1. Fitting Parameters for Wagner Model for Hydrated Milkweed PHTG

material	τ_p	G_p	K	a_1	a_2
milkweed	0.01	34351 ± 1000	0.0995 ± 0.03	0.256 ± 0.01	0.0079 ± 0.0008
PHTG	0.1	1101 ± 120			
	1	230 ± 20			
	10	221 ± 6			
	100	40 ± 2			
	1000	282 ± 10			

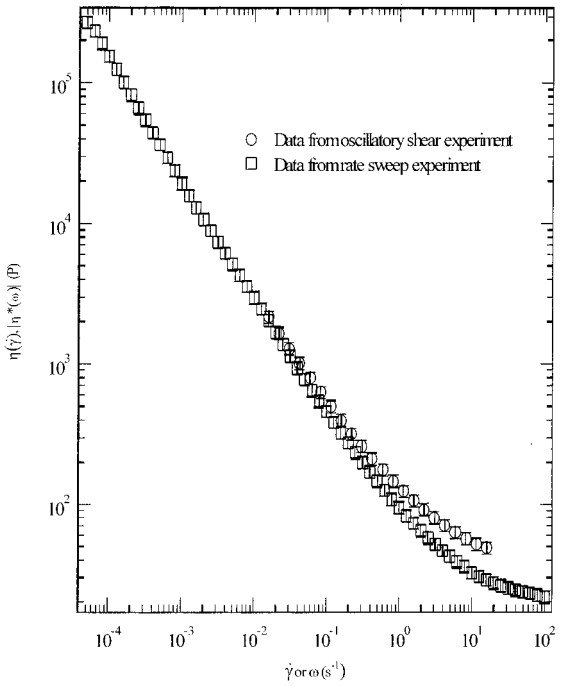

Figure 7. Cox–Merz plot for milkweed PHTG at 25 °C. Oscillatory data were obtained at an applied strain of 0.5%.

which describes the strain history imparted to the material, $m(t - t')$ is the memory function, t is the time, and $h(I_B,II_B)$ is the damping function which is expressed in terms of the first and second invariants of the Finger strain dyadic. In simple shear, the damping function becomes a function of the applied strain, γ. Implicit in the presentation of eq 1 is the assumption of strain−time separability, i.e., that the time and strain dependence of the material may be described using independent functions (*23*). The memory function in eq 1 may be expressed as a summation of exponentials in accord with the classic Maxwell model

$$m(t - t') = -\frac{\partial G(t - t')}{\partial t'} = \sum_p \frac{G_p}{\tau_p} e^{-(t-t')/\tau_p} \qquad (2)$$

where $G(t - t')$ is the linear stress relaxation modulus, and the set G_p and τ_p define the relaxation behavior of the material.

Application of eq 1 first requires that the relaxation function be determined from the linear VE regime. Once the linear VE region has been determined, the damping function can be evaluated from the ratio of the nonlinear stress relaxation modulus, $G(t - t',\gamma)$, to the linear stress relaxation modulus, $G(t - t')$

$$h(\lambda) = \frac{G(t - t',\gamma)}{G(t - t')} \qquad (3)$$

Many different forms have been advanced for the damping function by Wagner (*21, 22*), Soskey−Winter (*24*), and Laun (*25*) the most widely used, eqs 4, 5, and 6, respectively. These equations may be expressed as follows:

$$h(\gamma) = e^{-a\gamma} \qquad (4)$$

$$h(\gamma) = \frac{1}{1 - a\gamma^b} \qquad (5)$$

$$h(\gamma) = Ke^{-a_1\gamma} + (1 - K)e^{-a_2\gamma} \qquad (6)$$

where K, a, b, a_1, and a_2 are fitting parameters for the various formulations. For many synthetic polymer materials, the double exponential equation proposed by Laun has been used extensively to describe the nonlinear VE behavior of large strains. Once a damping function has been selected, and the linear VE behavior has been evaluated, the nonlinear behavior of the system can be predicted using eq 1.

Evaluation of the Linear Memory Function. To apply the Wagner model to predict the nonlinear VE properties of the hydrated milkweed PHTG suspension, the coefficients in the memory function (eq 2) need to be evaluated as discussed above. For the work reported herein, the coefficients for the memory function were evaluated by fitting the following equations

$$G(t - t') = \sum_p G_p e^{-(t-t')/\tau_p} \qquad (7)$$

$$G'(\omega) = \sum_p \frac{G_p(\omega\tau_p)^2}{1 + (\omega\tau_p)^2} \qquad (8)$$

to the stress relaxation and oscillatory shear flow data obtained in the linear VE range. In eq 8, $G'(\omega)$ is the linear oscillatory storage modulus. For the fits, the relaxation time constants, τ_p, were held constant in accord with the spacings of a Maxwell model, namely, 0.01, 0.1, 1, 10, 100, and 10^3 s. The values for G_p were selected to minimize the fitting error of the model to the data sets. The results of the fits along with the associated ± one sigma errors are summarized in **Table 1**.

Evaluation of the Damping Function. The damping function in the Wagner model can be determined from the ratio of the nonlinear stress relaxation modulus at a specific strain level to the linear stress relaxation modulus as described above. This procedure was used to evaluate the damping function for the hydrated milkweed PHTG suspension. Selection of the appropriate damping function is crucial to developing a constitutive equation that can predict adequately the nonlinear rheological behavior of a material. Three different forms for the damping function were evaluated, namely those proposed by Wagner, Soskey−Winter, and Laun (eqs 4, 5, and 6, respectively). The fits of the various damping functions to the data obtained for hydrated milkweed PHTG are illustrated in **Figure 8**. The Wagner formulation predicts a much more rapid decrease in the damping function with increasing strain in the nonlinear

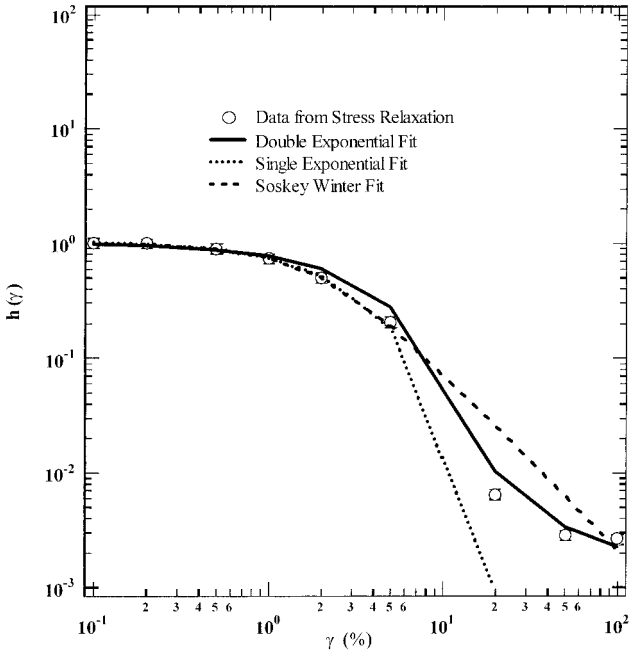

Figure 8. Evaluation of the damping function, $h(^{\circ}\gamma)$, for hydrated milkweed PHTG at 25 °C.

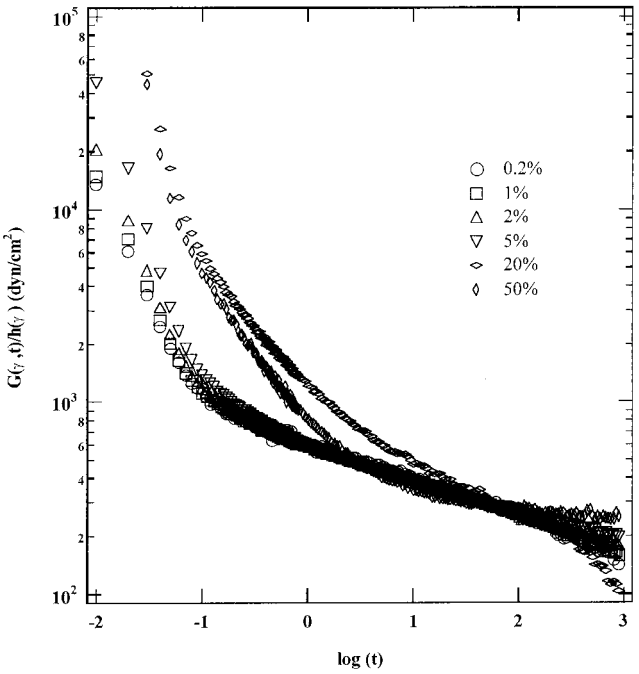

Figure 9. Effect of applied strain on the reduced stress relaxation modulus.

VE regime than is observed in the experimental data. In contrast, the Soskey−Winter damping function yields a weaker dependence on the applied strain than is observed experimentally. The Laun double exponential damping function provides an adequate description of the observed strain dependence.

In this work the Laun damping function was chosen to describe the effects of nonlinearity of the VE functions. The values obtained for the Laun damping function for the hydrated milkweed PHTG sample along with the associated ± one sigma errors are summarized in **Table 1**.

Validity of Time−Strain Separability Assumption. As mentioned above, an essential aspect of the Wagner model is the assumption of time−strain separability. Time−strain separability in rheological data may be examined by plots of $G(\gamma,t)/h(\gamma)$ versus the logarithm of time for each applied strain (*26*). Over the strain range that time−strain separability holds, the graphs should collapse to a single curve. Alternatively, a plot of $G(\gamma,t)/G(0,t)$ versus the applied strain should also collapse to a single curve over the strain range where time−strain separability is valid (*27*). A plot of $G(\gamma,t)/h(\gamma)$ versus logt is illustrated in **Figure 9**. From the data displayed in the figure it is evident that time−strain separability is valid for applied strains up to 20%. At higher strain levels, the assumption appears to break down.

Prediction of the Successive Start-up of Steady-State Shear. The results of a series of successive start-ups of steady-state shear flow are illustrated in **Figure 10**. The experiments were conducted at shear rates of 0.001, 0.01, 0.1, and 1 s^{-1} with hold times of 600 s. The experimental data at 0.001 and 0.01 s^{-1} do not display any stress overshoots.

At the lowest shear rate, 0.001 s^{-1}, the data appear to have not reached a stable plateau after 600 s. At the higher shear rates, namely, 0.1 and 1 s^{-1}, a small stress overshoot is observed after which the data decay quickly to a steady plateau.

For the start-up of steady-state shear flow the Wagner model may be expressed as

$$\eta^+(\dot{\gamma},t) = \int_0^t G(s)\left[s\frac{\partial h(s)}{\partial s} + h(s)\right]ds \qquad (9)$$

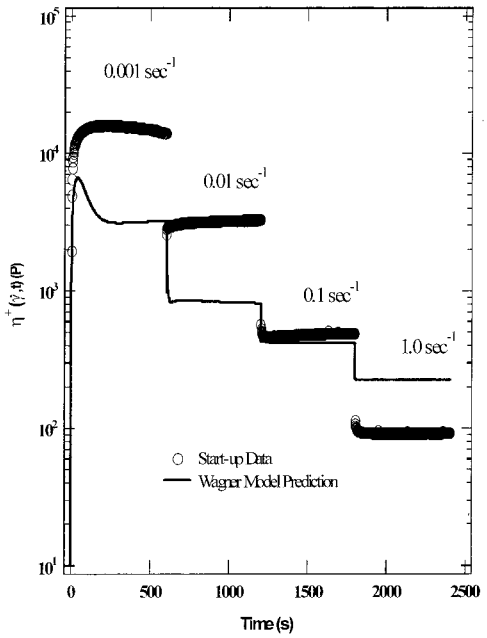

Figure 10. Prediction of the start-up of steady-state shear for hydrated milkweed PHTG using the Wagner model with a Laun damping function. Experimental data were obtained at 25 °C.

where $\eta^+(\dot{\gamma},t)$ is the shear stress growth coefficient, and $G(s)$ and $h(s)$ are defined in eqs 2 and 6, respectively. The prediction for the start-up of steady-state shear flow using the Wagner model at the various shear rates is displayed in **Figure 10**. At a shear rate of 0.001 s^{-1}, the model predicts a lower plateau viscosity then is observed experimentally. In addition, the model also predicts a pronounced stress overshoot which is not observed. At a shear rate of 0.01 s^{-1}, the model also predicts a lower plateau viscosity than is observed in the experiment. Both of these results are probably due to an over-estimation of the build-up of strain in the material via the damping function. At shear rates of 0.1 and 1 s^{-1}, the model accurately predicts the viscosity plateau and then over-predicts the plateau at the higher

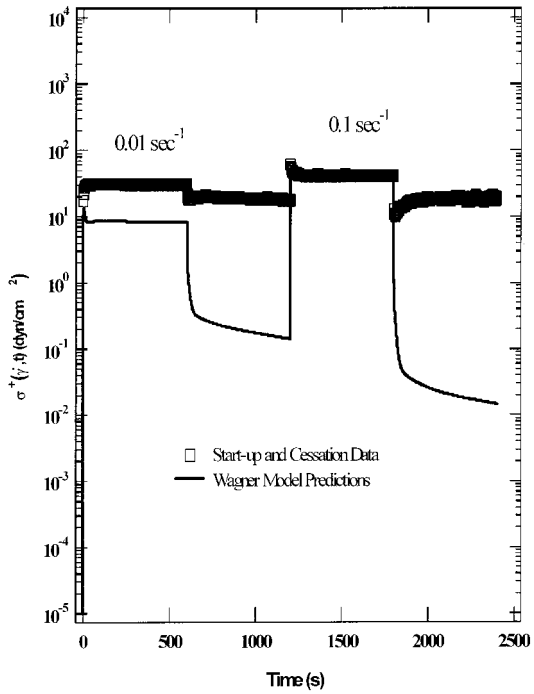

Figure 11. Prediction of the cessation of steady-state shear for hydrated milkweed PHTG using the Wagner model with a Laun damping function. Experimental data were obtained at 25 °C.

shear rate. At the high shear rates the damping function is underestimating the strain build-up in the material.

Prediction of the Cessation of Steady-State Shear. The results of a series of start-ups and subsequent cessations of steady-state shear flow are illustrated in **Figure 11**. The data were collected at 0.01 and 0.1 s^{-1} with hold times of 600 s. The experimental data obtained at 0.01 s^{-1} do not display any evidence of a stress overshoot, whereas the data obtained at 0.1 s^{-1} do display a slight stress overshoot. After each start-up experiment, the flow was halted for 600 s and the response of the system was followed. During both periods of cessation the fluid displayed very slight relaxation indicating the presence of long relaxation times. From **Figure 6**, the presence of a plateau region at low shear rates may be observed in both the linear and nonlinear VE regimes. The presence of this plateau is another indication of the existence of long relaxation times for the material which may be due to a transient network in the fluid from association of the hydrated milkweed PHTG macromolecules.

For cessation of steady-state shear flow, the Wagner model may be expressed as

$$\sigma^{-}(\dot{\gamma},t) = \dot{\gamma}_{cess}\int_{t}^{t+t_{cess}} G(s)\left[(s-t)\frac{\partial h(s)}{\partial s} + h(s)\right]ds \quad (10)$$

where $\sigma^{-}(\dot{\gamma},t)$ is the shear stress decay function, $\dot{\gamma}_{cess}$ is the shear rate which is applied to the sample prior to cessation, and t_{cess} is the time the shear rate is applied prior to cessation. The corresponding shear stress growth function predicted by the Wagner model during the start-up of steady-state shear may be obtained from the shear stress growth coefficient given by eq (7) using $\sigma(\dot{\gamma},t) = \eta^{+}(\dot{\gamma},t)\dot{\gamma}_{cess}$.

The predictions of the Wagner model for the cessation of steady-state shear flow are illustrated in **Figure 11**. For the hydrated milkweed PHTG sample, the model predictions for the start-up of steady-state shear data have been discussed above. At both of the shear rates displayed in **Figure 10**, 0.01 and 0.1 s^{-1}, the Wagner model predicts a rapid decrease in the shear stress decay function which is not observed experimentally. The experimental data display only a slight degree of relaxation which may be indicative of a transient network as discussed above. Because the stress relaxation curves at the various applied strains did not give an indication of a stable network, the model predictions will not contain any network-like behavior and, thus, over-predict the decrease in the shear stress decay function.

ACKNOWLEDGMENT

We thank Mr. A. J. Thomas for conducting many of the rheological experiments.

LITERATURE CITED

(1) Harry-O'kuru, R. E.; Mojtahedi, H.; Vaughn, S. F.; Dowd, P. F.; Santo, G. S.; Holser, R. A.; Abbott, T. P. Milkweed seed meal: A control for *Meloidogyne chitwoodi* on potatoes. *Ind. Crops Prod*. **1999**, *9*, 145−150.

(2) Phillips, B. S.; Fries, R. D.; Rennick, K. A.; Abbott, T. P. A comparison of the chemical properties of Asclepias seed oil stored under various conditions. In *Abstracts from the Annual Meeting, Association for the Advancement of Industrial Crops*, 1996; p 13.

(3) Harry-O'kuru, R. E.; Abbott, T. P. Cardenolide analysis of cold-pressed milkweed oil. *Ind. Crops Prod*. **1997**, *7*, 53−58.

(4) Schmitz, W. R.; Wallace, J. G. Epoxidation of methyl oleate with hydrogen peroxide. *J. Am. Oil Chem. Soc*. **1954**, *31*, 363−365.

(5) Chadwick, A. F.; Barlow, D. O.; D'Addieco, A. A.; Wallace, J. G. Theory and practice of resin-catalyzed epoxidation. *J. Am. Oil Chem. Soc*. **1958**, *35*, 355−358.

(6) Rusling, J. F.; Riser, G. R.; Snook, M. E.; Scott, W. E. Epoxidation of alkyl esters of 12,13-epoxyoleic acids and evaluation of diepoxides as plasticizers for poly(vinyl chloride). *J. Am. Oil Chem. Soc.* **1968**, *45*, 760−763.

(7) Meffert, A. Technical uses of fatty acid esters. *J. Am. Oil Chem. Soc*. **1984**, *61*, 255−258.

(8) Barrett, L. W.; Sperling, L. H.; Murphy, C. J. Naturally functionalized triglyceride oils in interpenetrating polymer networks. *J. Am. Oil Chem. Soc*. **1993**, *70*, 523−534.

(9) Dahlke, B.; Hellbardt, S.; Paetow, M.; Zech, W. H. Polyhydroxy fatty acids and their derivatives from plant oils. *J. Am. Oil Chem. Soc*. **1995**, *72*, 349−353.

(10) Ayorinde, F. O.; Butler, B. D.; Clayton, M. T. *Vernonia galamensis*: a rich source of epoxy acid. *J. Am. Oil Chem. Soc*. **1990**, *67*, 844−845.

(11) Carlson, K. D.; Kleiman, R. Lesquerella as a source of hydroxy fatty acids for industrial products. *Growing Industrial Materials Series, U. S Department of Agriculture, Cooperative State Research Service in conjunction with the Agricultural Research Service, Economic Research Service and University of Missouri*; October, 1991.

(12) Harry-O'kuru, R. E.; Holser, R. A.; Abbott, T. P.; Weisleder, D. Synthesis and characteristics of polyhydroxy triglycerides from milkweed oil. *Ind. Crops Prod.* **2002**, *15*, 51−58.

(13) Findley, T. W.; Swern, D.; Scalan, J. T. Epoxidation of unsaturated fatty materials with peracetic acid in glacial acetic acid. *J. Am. Chem. Soc*. **1945**, *67*, 412−414.

(14) Frykman, H. B.; Isbell, T. A. Synthesis of 6-hydroxylactones and 5,6-dihydroxy eicosanoic acids from meadowfoam fatty acids via a lipase-medeated self-epoxidation. *J. Am. Oil Chem. Soc.* **1997**, *74*, 719−722.

(15) Rusch gen Klaas, M.; Warwel, S. Chemoenzymatic epoxidation of unsaturated fatty acid esters and plant oils. *J. Am. Oil Chem. Soc*. **1996**, *73*, 1453−1457.

(16) Page-Xatart-Pares, X.; Bonnet, C.; Morin, O. Synthesis of new derivatives from vegetable oil methyl esters via epoxidation and oxirane ring opening. In *Recent Developments in the Synthesis of Fatty Acid Derivatives*; Knothe, G., Derksen, J. T. P, Eds.; JAOC: Champaign, IL, 2000; pp 141−156.
(17) Gunstone, F. D. The study of natural epoxy oils and epoxidized vegetable oils by 13C nuclear magnetic resonanace spectroscopy, *J. Am. Oil Chem. Soc*. **1993**, *70*, 1139−1144.
(18) Whistler, R. L. Factors influencing gum costs and applications. In *Industrial Gums, Polysaccharides and their Derivatives*, 2nd ed.; Whistler, R. L., BeMiller, J. N., Eds.; Academic Press: New York and London, 1973; pp 13−14.
(19) Cox, W. P.; Merz, E. H. Correlation of dynamic and steady flow viscosities, *J. Polym. Sci*. **1958**, *28*, 619−622.
(20) Bernstein, B. E.; Kersley, A.; Zapas, L. J. A theory of stress relaxation with finite strain. *Trans. Soc. Rheol*. **1963**, *7*, 391−410.
(21) Wagner, M. H. Analysis of time-dependent nonlinear stress-growth data for shear and elongational flow of low-density branched polyethylene melt. *Rheol. Acta* **1976**, *15*, 136−142.
(22) Wagner, M. H. A constitutive analysis of uniaxial elongational flow data of a low-density polyethylene melt. *J. Non-Newt. Fluid Mech*. **1978**, *4*, 39−55.
(23) Zapas, L. J.; Croft, T. Correlation of large longitudinal deformations with different strain histories. *J. Res. Nat. Bur. Stand. (U. S.)* **1965**, *69A*, 541−546.
(24) Soskey, P. R.; Winter, H. H. Large step strain experiments with parallel-disk rotational rheometers. *J. Rheol*. **1984**, *28*, 625−645.
(25) Laun, H. M. Description of the nonlinear shear behavior of a low density polyethylene by means of an experimentally determined strain dependent memory function. *Rheol. Acta* **1978**, *17*, 1−15.
(26) Osaki, K.; Nishizawa, K.; Kurata, M. Material time constant characterizing the nonlinear viscoelasticity of entangled polymer systems. *Macromolecules* **1982**, *15* (5), 1068−1071.
(27) Rouiller, V., McKenna, G. B. A hybrid nonlinear constitutive model: comparisons with multistep data for a polyurethane rubber. In *Conference Proceedings at ANTEC 98*; Society of Plastics Engineers: Brookfield, CT, 1998; vol. 2, pp 2138−2142.

Received for review November 5, 2001. Revised manuscript received March 15, 2002. Accepted March 16, 2002. Names are necessary to report factually on available data; however, the USDA neither guarantees nor warrants the standard of the product, and the use of the name by USDA implies no approval of the product to the exclusion of others that may also be suitable.

JF011464Z